Journal of Nuclear Materials 407 (2010) 126–135

Contents lists available at ScienceDirect

Journal of Nuclear Materials

journal homepage: www.elsevier.com/locate/jnucmat

Correlation of the thermodynamic calculation and the experimental observation of Ni–Mo–Cr low alloy steel changing Ni, Mo, and Cr contents

Sang-Gyu Park [a,*], Min-Chul Kim [b], Bong-Sang Lee [b], Dang-Moon Wee [a]

[a] Korea Advanced Institute of Science and Technology, 373-1 Guseong-dong, Yuseong-gu, Daejeon 305-701, Republic of Korea
[b] Korea Atomic Energy Research Institute, 150 Deogjin-dong, Yuseong-gu, Daejeon 305-353, Republic of Korea

ARTICLE INFO

Article history:
Received 19 June 2009
Accepted 6 September 2010

ABSTRACT

SA508 Gr.4N Ni–Mo–Cr low alloy steel has improved fracture toughness and strength compared to commercial low alloy steels such as SA508 Gr.3 Mn–Mo–Ni low alloy steel, which has less than 1% Ni. Higher strength and fracture toughness of low alloy steels can be achieved by increasing the Ni and Cr contents. In this study, the effects of the alloying elements of Ni and Cr on the microstructural characteristics and mechanical properties of SA508 Gr.4N Ni–Mo–Cr low alloy steel are evaluated. Changes in the stable phases of SA508 Gr.4N low alloy steel with these alloying elements were evaluated using thermodynamic calculation software. These values were then compared with the observed microstructural results. Additionally, tensile tests and Charpy impact test were carried out to evaluate the mechanical properties. The thermodynamic calculations show that Ni mainly affects the change of the matrix phase of γ and α rather than the carbide phase. Contrary to the Ni effect, Cr and Mo primarily affect the precipitation behavior of the carbide phases of $Cr_{23}C_6$, Cr_7C_3 and Mo_2C. In the microscopic observations, the lath martensitic structure becomes finer as the Ni content increases without affecting the carbides. When the Cr content decreases, the Cr carbide becomes unstable and carbide coarsening occurs. Carbide Mo_2C in the form of fine needles were observed in the high-Mo alloy. Greater strength was obtained after additions of Ni and Mo and the transition properties were improved as the Ni and Cr contents increased. These results were correlated with the thermodynamic calculation results.

Contents

1. Introduction

Low alloy steels, used for nuclear pressure vessels, steam generators and in other applications, constitute a large fraction of the materials used in nuclear power plants. In this regard, they are very important materials in that they determine the safety and the life span of nuclear power plants [1–5]. Currently, nuclear power plants are being built on a larger scale to raise their power generation efficiency. However, if commercial pressure vessel steels are used in a larger pressure vessel, it is necessary to increase the thickness of these components to satisfy the required

* Corresponding author.
E-mail address: sg121243@kaist.ac.kr (S.-G. Park).

0022-3115/$ - see front matter © 2010 Elsevier B.V. All rights reserved.
doi:10.1016/j.jnucmat.2010.09.004

endurance strength. However, increasing the thickness may cause productivity and weldability problems. To solve these problems, nuclear pressure vessel steel should be stronger than SA508 Gr.3 commercial pressure vessel steel. Moreover, considering the loss of toughness due to the weakening effects of neutron irradiation during long-term operation, improving the toughness is very important when a pressure vessel is initially fabricated.

It is known that a higher strength and fracture toughness of low alloy steels can be achieved by increasing the Ni and Cr contents [6]. SA508 Gr.4N Ni–Mo–Cr low alloy steel, which has higher Ni and Cr contents compared to SA508 Gr.3 Mn–Mo–Ni low alloy steel, also has much better mechanical properties. Ni is an element that effectively enhances the strength and toughness. Moreover, the addition of these types of elements increases the hardenability of a low alloy steel. Therefore, the microstructure of SA508 Gr.4N low alloy steel after quenching is a mixture of martensite and lower bainite microstructures. These microstructural changes cause an improvement in the mechanical properties. In spite of the superior mechanical properties of SA 508 Gr.4N Ni–Mo–Cr low alloy steel, it has yet to be used in a commercial nuclear power plant, as Ni is considered to be an element that is susceptible to irradiation, not unlike Cu [7,8]. However, the greater strength and toughness from steels that contain Ni is very attractive to those that require RPV steel. As a result, several researchers have investigated the potential use of SA508 Gr.4N low alloy steel in NPP applications. For this reason, the design of optimum chemical compositions within the ASME specification of SA508 Gr.4N low alloy steel is required. In order to achieve the optimum composition, it is necessary to study alloying effects in SA508 Gr.4N low alloy steel.

In this study, the effects of three alloying elements (Ni, Cr and Mo) on the mechanical properties of Ni–Mo–Cr low alloy steels are systematically investigated. Thermodynamic calculation is a well-known efficient method [9] in the design of an alloy. In this study, thermodynamic calculations were carried out to estimate the stable phase and its fraction. The microstructures of the model alloys were then examined and compared with the results of the thermodynamic calculations. The tensile properties and ductile–brittle transition behaviors were also characterized according to the alloying element type and amounts. Based on the microstructure/mechanical property relationships obtained from the literature and from experimental works on SA508 Gr.4N Ni–Mo–Cr low alloy steels, and with correlations with the results of the thermodynamic calculations, fundamental information regarding alloy designs is discussed.

2. Experimental details

The chemical compositions of the model alloys used in this study are given in Table 1. A model alloy, K4-Ref, with the typical composition of SA508 Gr.4N steel as described within the ASME specified composition, was prepared as a reference alloy. In order to characterize the effect of each element quantitatively, ingots of the model alloys were prepared with various Ni, Cr and Mo contents. The heat treatment condition for the model alloys is described in Table 2.

Table 1
Chemical compositions of model alloys (wt%).

	C	Mn	Ni	Cr	Mo	P	S	Fe
K4-Ref	0.19	0.29	3.59	1.79	0.49	0.002	0.002	Bal.
K4-Ni1	0.21	0.33	2.66	1.81	0.53	0.002	0.002	Bal.
K4-Ni2	0.20	0.35	4.82	1.83	0.53	0.002	0.002	Bal.
K4-Cr1	0.21	0.32	3.65	1.04	0.54	0.002	0.002	Bal.
K4-Cr2	0.21	0.32	3.63	2.47	0.53	0.002	0.002	Bal.
K4-Mo1	0.20	0.33	3.57	1.87	0.10	0.002	0.002	Bal.
K4-Mo2	0.20	0.32	3.70	1.86	1.02	0.002	0.002	Bal.

Table 2
Heat treatment condition.

Heat treatment	Homogenization	Austenitizing	Tempering
Condition (°C, h)	1200 °C, 10 h/FC[a]	880 °C, 2 h/AC[b]	660 °C, 10 h/FC[a]

[a] FC: Furnace cooling.
[b] AC: Air cooling.

Microstructure observations were made using an optical microscope and a scanning electron microscope (SEM). Specimens for these observations were prepared by grinding and polishing up to 0.25 μm followed by etching in a 3% Nital solution. To investigate the overall distribution of the carbides and to analyze the individual carbide particles in detail, a carbon extraction replica technique was employed. Carbon extraction replicas were examined using a JEOL JEM-2000FX2 and a FB-2100F transmission electron microscope. To evaluate the changes in the stable phases and related fractions depending on the content of the alloying elements, thermodynamic calculations were carried out using Thermo-Calc Classic version R from Thermocalc with the TCFE5 database.

The tensile properties of the alloys were evaluated using a MTS universal static testing machine at a stain rate of 1.11×10^{-3}/s at room temperature. The yield strength was determined by a 0.2% strain offset stress, or by the lower yield stress. Impact energy transition curves were obtained using standard Charpy V-notched specimens in accordance with ASTM E23. Impact tests were conducted using the SATEC-S1 impact test machine with a maximum capacity of 406 J in a temperature range of −196 °C to 100 °C. The index temperatures were determined from fitted Charpy curves as the temperature corresponding to the Charpy energy values of 41 J and 68 J.

3. Results and discussion

3.1. Thermodynamic calculation for stable phase with alloy composition

Fig. 1 shows the results of the thermodynamic calculations for K4-Ref, K4-Ni1, and K4-Ni2. The austenite phase region was extended toward a low temperature range, which indicates that the fraction of austenite increased due to the stabilization effect of austenite [10]. However, it was found that an addition of Ni does not significantly affect the formation of carbide. There were no changes observed in the carbide phase region between K4-Ni1, K4-Ref and K4-Ni2.

Fig. 2a shows the calculation result for K4-Cr1, which has a lower Cr content than K4-Ref. In this case, the stable $M_{23}C_6$ and M_7C_3 phase in the range of 600–700 °C became unstable and the fractions of $M_{23}C_6$ and M_7C_3 were decreased with a decrease in the temperature, whereas the fraction of the $M_{23}C_6$ phase in K4-Ref remained constant over the entire temperature range. However, upon the addition of more Cr, as was done with K4-Cr2, a significant difference in the precipitation behavior was not noted in K4-Ref. In addition, the austenite region was reduced in the low temperature range. This may have been caused by a change of the fractions of the carbide phases in the model alloy. As the fractions of the carbides are decreased, the fraction of the other phase (austenite) will increase as a result.

The calculation results as the Mo contents varied are presented in Fig. 3. This figure shows that the addition of Mo into SA508 Gr.3 Mn–Mo–Ni low alloy steel promotes the precipitation of fine needle-type M_2C [11]. In the case of SA508 Gr.4N Ni–Mo–Cr low alloy

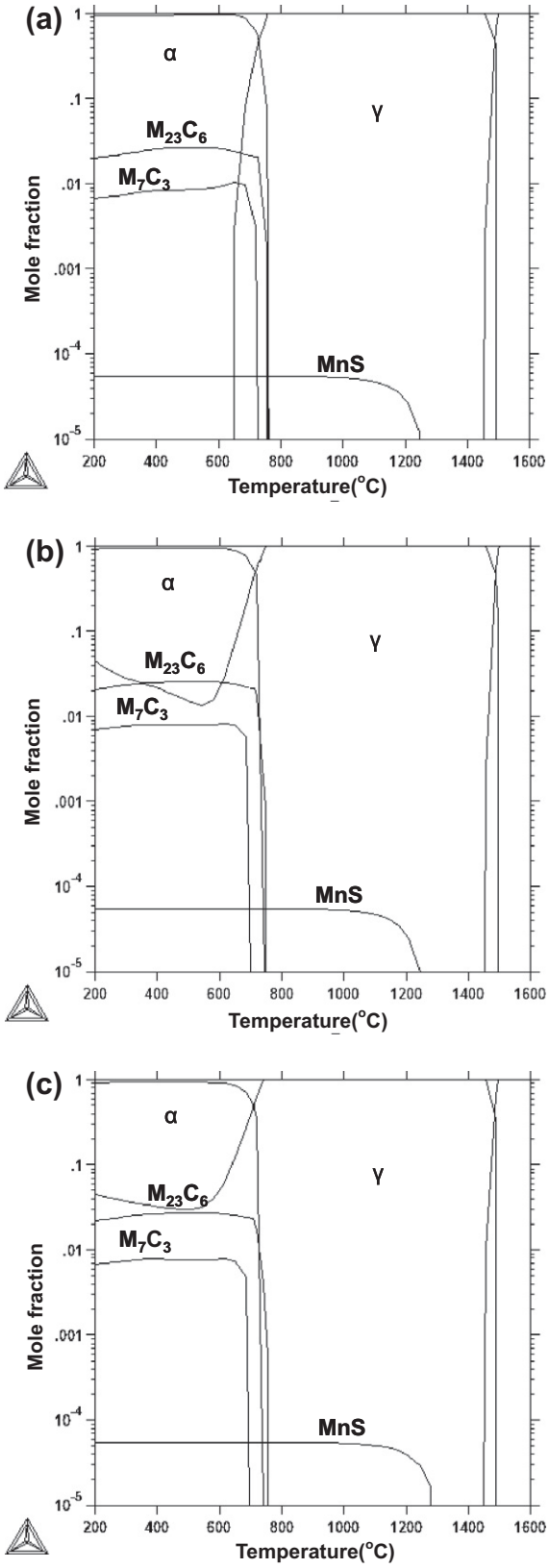

Fig. 1. Thermodynamic calculation results of: (a) K4-Ni1, (b) K4-Ref and (c) K4-Ni2.

steel, remarkable changes were observed in terms of the formation of stable carbide. It was predicted in the calculation that M2C would not be precipitated in the cases of K4-Ref and K4-Mo1, which have lower Mo contents, whereas it was precipitated at

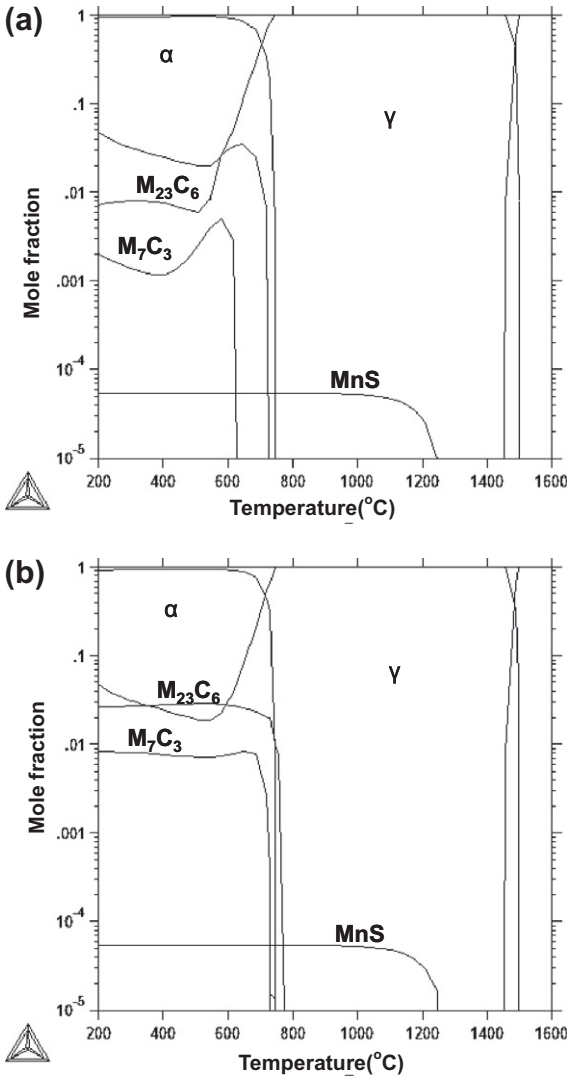

Fig. 2. Thermodynamic calculation results of: (a) K4-Cr1, (b) K4-Cr2.

approximately 600 °C in K4-Mo2. Instead, K4-Mo2 did not show the M_7C_3 phase over the entire temperature region. In addition, the amount of M_7C_3 was much higher than that of $M_{23}C_6$ in K4-Mo1 compared to K4-Ref. This result shows that M_7C_3 becomes unstable as the Mo content increases. Therefore, the addition of Mo suppresses the precipitation of the M_7C_3 phase and enhances the fractions of $M_{23}C_6$ and M_2C in the calculation results.

3.2. Microstructural changes with alloying elements

Scanning electron microscope (SEM) images of model alloys with different Ni contents are presented in Fig. 4. K4-Ref and K4-Ni2 have a mixture of tempered martensite and lower bainite structures, which is the typical microstructure of SA508 Gr.4N Ni–Mo–Cr low alloy steel. However, as the Ni content increases, the subgrains of the ferrite packets become finer, as shown in Fig. 4. It is generally known that Ni increases the hardenability of steels, which implies the ability of steel to form martensite upon quenching. Thus, an increased fraction of martensite can be obtained via the addition of Ni. It has been reported that the size of the bainite sheaf is two or three times larger than that of the martensite packet [12]. Therefore, it is likely that the fractions of martensite will be significantly increased with an addition of Ni and

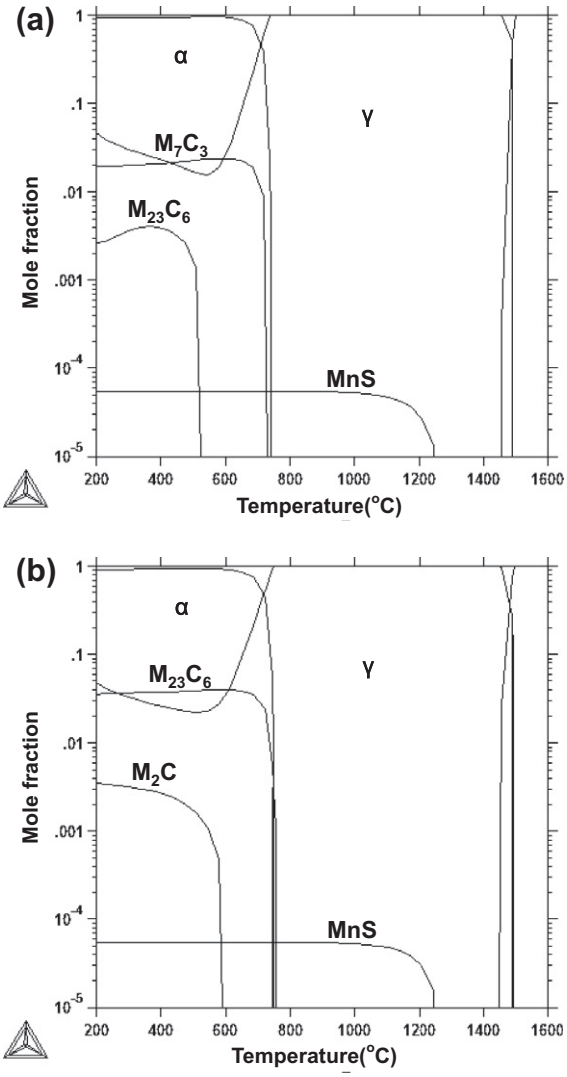

Fig. 3. Thermodynamic calculation results of: (a) K4-Mo1 and (b) K4-Mo2.

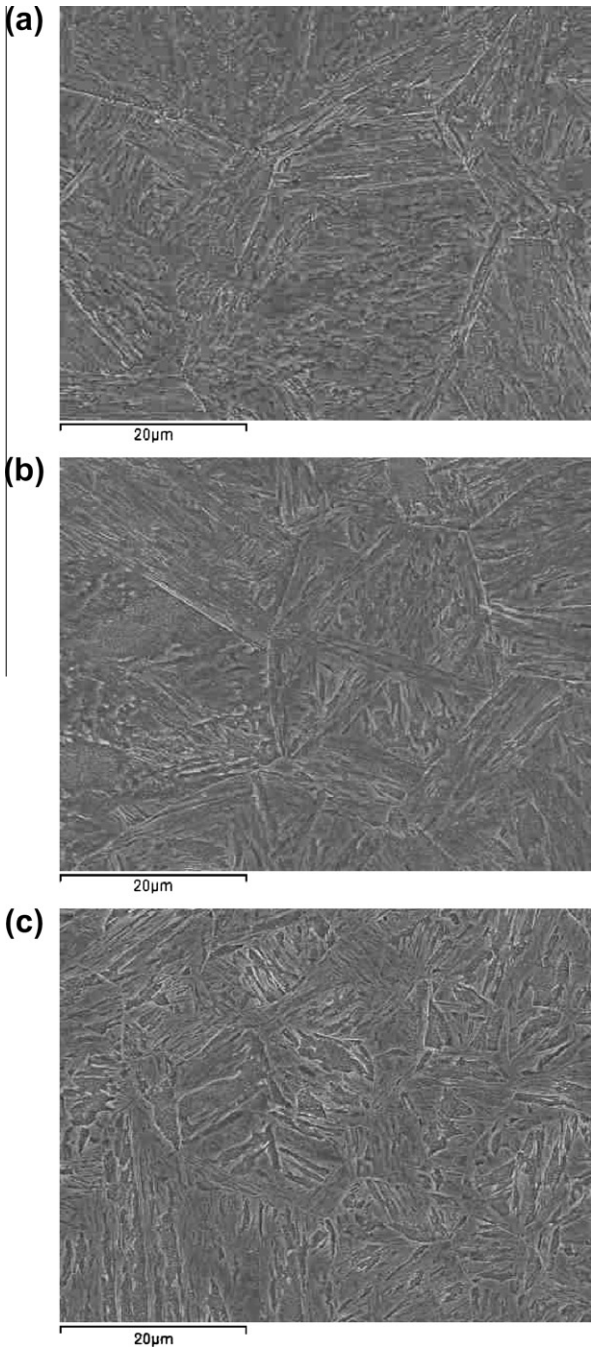

Fig. 4. SEM images of: (a) K4-Ni1, (b) K4-Ref and (c) K4-Ni2.

that this will reduce the size of the subgrains after the tempering process. In fact, the sizes of the subgrains decreased with an increase of the Ni contents. The grain refinement effect of Ni was reported previously [13,14], and the change in the microstructure with different Ni contents may be caused by a combination of the grain refinement and increased hardenability of Ni [15]. In contrast, there were no noticeable differences in the morphology and distribution behavior of the precipitates, even when observed by TEM. This finding is in very good agreement with the thermodynamic calculations.

In the case of model alloys with different Cr contents, changes in the carbide precipitation of $M_{23}C_6$ and M_7C_3 were investigated, as the calculation results suggested that the carbide phases would change significantly with variations in the Cr content. In order to observe the changes in the precipitation behavior with the Cr content, microstructure characterizations were carried out using transmission electron microscopy (TEM). Fig. 5 shows the distribution of the precipitates in thin foil specimens with different Cr contents. Relatively coarse carbides were observed in the K4-Cr1 (1.0 wt% Cr) which were not distributed evenly, whereas small carbides were observed to be distributed homogeneously in K4-Ref (1.8 wt% Cr) and K4-Cr2 (2.5 wt% Cr). To characterize the carbide distributions of the model alloys more accurately, a quantitative analysis of the carbides was conducted using an image analyzer. The result of this analysis is presented in Fig. 6. As shown in Fig. 6a–c, the size of the carbide decreased with an increase of the Cr content. The mean carbides size of the K4-Cr1, K4-Ref and K4-Cr2 are 0.408 μm, 0.312 μm and 0.267 μm, respectively. In addition, the mean size of the carbides above the top 1%, 5%, and 10% are summarized in Fig. 6d where the coarse carbides of each model alloy were compared. According to this result, significant carbide coarsening occurred in K4-Cr1. In the low-Cr alloy, the thermodynamic calculation result revealed that the amount of chromium carbide decreased at approximately 420 °C. Therefore, the Cr carbide becomes unstable and then dissolves into matrix under this temperature. Excessive carbon produced by carbide dissolution diffused into the neighboring carbide and coarsening occurred, as shown in Fig. 5. The fractions of the carbide phases re-

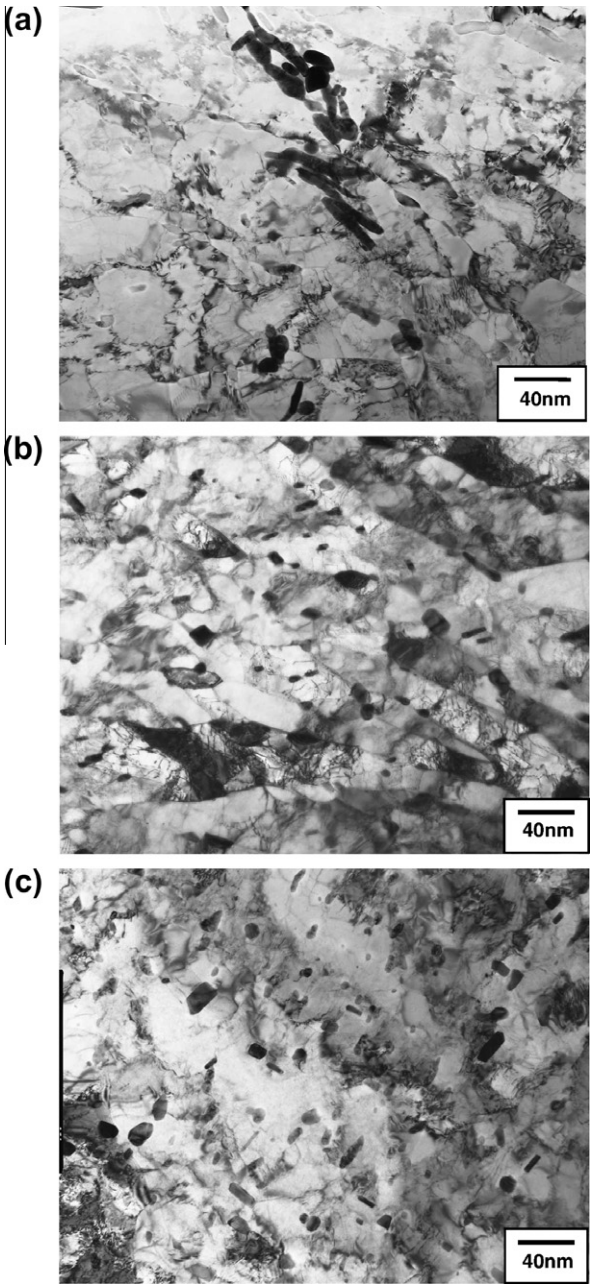

Fig. 5. Carbide distribution observed by TEM: (a) K4-Cr1, (b) K4-Ref and (c) K4-Cr2.

mained unchanged in these two model alloys in the thermodynamic calculations. However, additional Cr increases the possibility of carbide nucleation; thus, more carbides are present in the K4-Cr2 than in K4-Ref but are smaller due to the equivalent fraction of the carbide phase.

Fig. 7 shows the precipitate distribution in the thin foil specimens of K4-Mo1 (0.1 wt% Mo) and K4-Mo2 (1.0 wt% Mo). K4-Mo1 (0.1 wt% Mo) shows similar precipitation characteristics to K4-Ref (0.5 wt% Mo), whereas fine needle-type carbides are observed in K4-Mo2 (1.0 wt% Mo). To identify the carbides of the model alloys, selective area diffraction patterns of the carbides were obtained from the TEM images. These are shown in Fig. 8. The globular-type carbide is identified as chromium carbide $M_{23}C_6$, which has an FCC structure, and the parallelogram-shaped carbide is M_7C_3-type chromium carbide with an HCP structure. Generally, most of the precipitates in the model alloys are chromium carbide. However, the needle-type carbide observed in the K4-Mo2 specimen was too small to facilitate observation of the selective area diffraction pattern directly. For this reason, a diffraction pattern was analyzed from a high-resolution image via Fourier transformation [16], as shown in Fig. 9. Based on the diffraction pattern and on the results of prior research [17], this type of precipitate with an HCP structure is M_2C, which is molybdenum carbide. It can be concluded that the main precipitates types in K4-Mo2 (1. 0wt% Mo) are both chromium carbide of the $M_{23}C_6$ type and molybdenum carbide of the M_2C type.

From the results of the thermodynamic calculations and from microscopic observation, the microstructures of the model alloys show a very similar tendency with the calculation results. Therefore, 10 h of tempering time seems to be enough to build stabilized microstructure. In addition, the following effects of alloying elements on the precipitation behavior of SA508 Gr.4N Ni–Cr–Mo low alloy steel were deduced from the calculation and observation results.

(1) Ni refines the sizes of both prior austenite grains and the martensitic structure. It also increases the fraction of martensite after quenching. However, it does not affect the precipitation behavior.
(2) An addition of Cr enhances the precipitation of the $M_{23}C_6$ and M_7C_3 carbides considerably, and carbide coarsening is observed in the low-Cr model alloy.
(3) Additional Mo promotes the formation of the fine needle-type carbide (M_2C) instead of chromium carbide M_7C_3.

3.3. Tensile properties

Fig. 10 shows the tensile test results of the model alloys. The test results were also described in Table 3. In the model alloys with different Ni contents, the yield strength of K4-Ni1 (2.5 wt% Ni) was decreased by 50 MPa as compared to 580 MPa in K4-Ref (3.5 wt% Ni), and that of K4-Ni2 (4.5 wt% Ni) was increased to 680 MPa. Consequently, the strength was increased with an increase in the Ni content. A similar tendency in the strength was observed in the model alloys with different Mo contents. In this case, the yield strengths of the K4-Mo1, K4-Ref and K4-Mo2 specimens were 530 MPa, 580 MPa and 650 MPa, respectively. In general, it is known that Ni and Mo create a solid solution with a ferrite single phase which brings about a solid solution strengthening effect in steel. Moreover, it has been reported that the solid solution strengthening is proportional to the concentration [18,19]. In the concentration range of 2.5–3.5 wt% Ni, it appeared that the yield strength of model alloys were mainly affected by solid solution strengthening of Ni. However, there is more of an increment of the yield strength compared to what was expected by solid solution strengthening when the content of Ni exceeds 3.5 wt%. As observed earlier, the sizes of the grains decreased with an increase of the Ni content. In addition, the fractions of the martensite, with its higher yield strength compared to lower bainite, [12] increased in the K4-Ni2 specimen. Consequently, the reduced grain size and the increased fraction of martensite cause the additional strengthening effect in K4-Ni2. In the case of the model alloys with different Mo contents, the yield strengths of the model alloys changed linearly. This is also affected by the solid solution strengthening of Mo. Moreover, small needle-type carbide M_2C as observed in K4-Mo2 also increases the yield strength of the steel due to its precipitation strengthening effect [11,20].

On the other hand, only slight changes were observed in the yield strength as the Cr content varied. Compared to K4-Ref (1.8 wt% Cr), the differences in the yield strengths of the model alloys with different Cr contents were less than 10 MPa. The thermodynamic calculation result confirmed that the addition of Cr

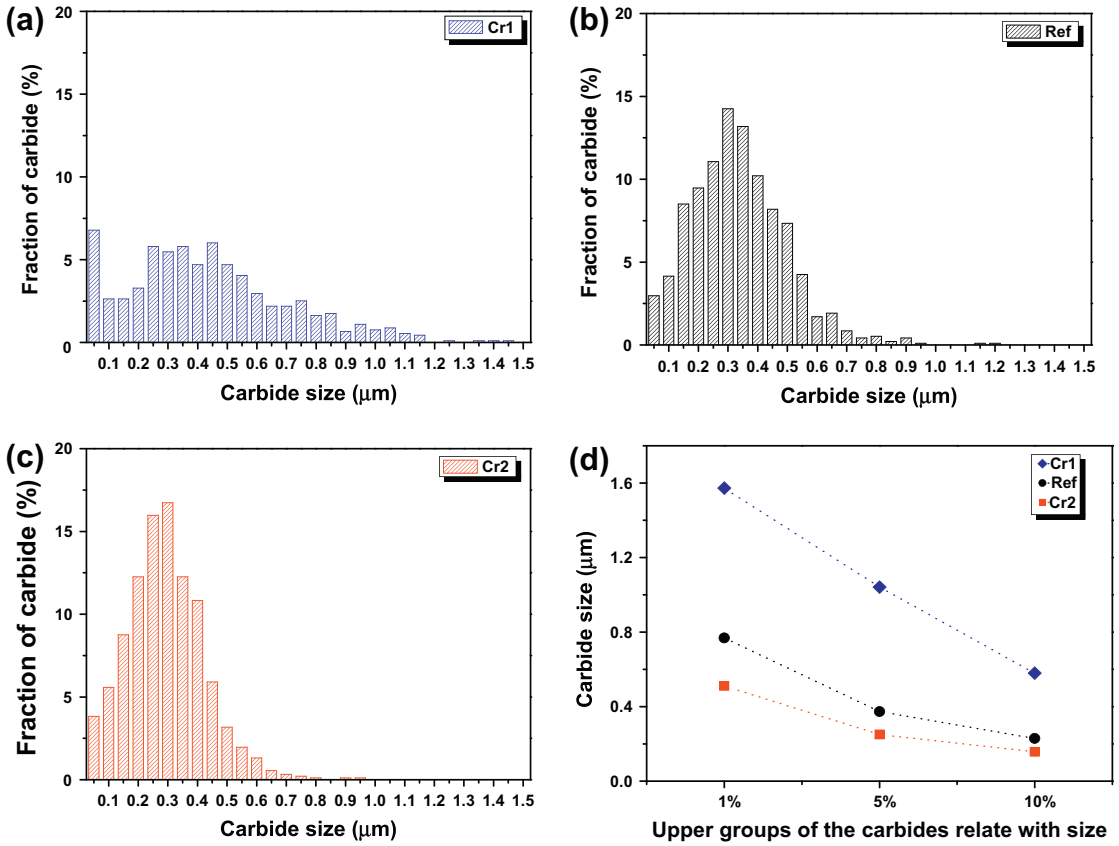

Fig. 6. Carbide size of the model alloys: (a) K4-Cr1, (b) K4-Ref, (c) K4-Cr2 and (d) in the top 1%, 5% and 10%.

increased the formation of chromium carbides in the SA508 Gr.4N low alloy steel. Thus, the amount of Cr solved into the steel may be lower than that added to the steel. Therefore, the solid solution hardening effect of Cr would be smaller than that of Ni or Mo. The shapes of the Cr carbides are globular and have no orientation relationship with the matrix; consequently, they do not have a precipitation strengthening effect [21]. In conclusion, the change of the carbide distribution with different levels of Cr does not affect the strength of SA508 Gr.4N low alloy steel.

3.4. Transition behavior

The Charpy impact test results are shown in Fig. 11. The index temperatures and upper shelf energies were presented in Table 3. In Fig. 11a, K4-Ni1 (2.5 wt% Ni) showed the highest index temperature, T_{41J}. It was elevated 40 °C more than the −127 °C reading of K4-Ref (3.5 wt%), whereas the T_{41J} value of K4-Ni2 (4.5 wt% Ni) is lower by 25 °C compared with that of K4-Ref (3.5 wt%). Many researchers have reported that additional Ni increases the toughness of low alloy steel [12,15,22–26]. One cause of this improvement due to the addition of Ni is the refinement of the martensite packets. It is generally known that the toughness of the tempered martensitic steel is largely affected by the size of the martensite packets and laths. As was mentioned in Section 3.2, an addition of Ni enhances the ability of the steels to harden, which increases the martensite fraction and packet size reduction [12,15]. The tendency of the packet size refinement by Ni addition is also shown in Fig. 4. However, the size of the laths did not change much with the increase in Ni contents in the TEM observation. Therefore, the reduced packet size may cause the model alloys to improve in toughness [23]. Moreover, it has been reported that an addition of Ni affects the ability of the dislocations to cross slip in the bcc iron lattice and makes these cross slips easier [24]. Fig. 11b shows the Charpy impact test result of the K4-Cr1, K4-Ref and K4-Cr2 specimens. K4-Cr1 (1.0 wt% Cr) shows the lowest Charpy impact properties. Its index temperature, T_{41J}, was elevated by nearly 60 °C relative to the −127 °C reading of K4-Ref (1.8 wt% Cr), and the Upper shelf energy (USE) value was decreased by 30 J from the 224 J value of K4-Ref. The transition temperatures also decreased with the addition of Cr. This result may have resulted from the difference in the carbide distribution behavior. As observed earlier, the Cr carbides of $M_{23}C_6$ and M_7C_3 were coarsened in K4-Cr1. It has been reported that coarse carbides can cause a decrease in the Charpy impact characteristics [27]. Additional Cr over 1.8 wt% in the model alloys improves Charpy impact properties. This result also can be explained in terms of the carbide size refinement with an increase of the Cr content. Thus, the smaller carbides in K4-Cr2 compared to those of K4-Ref may have improved the transition behavior in the model alloys. The Charpy impact properties with differing amounts of Mo are shown in Fig. 11c. In general, T_{41J} increased as the Mo content increased. The T_{41J} value of K4-Mo2 (1.0 wt% Mo) was elevated by nearly 10 °C while the USE value was reduced by 40 J compared to those values of K4-Ref (0.5 wt% Mo). The toughness of K4-Mo1 (0.1 wt% Mo) showed a slight improvement. Though the addition of Mo was effective in improving the strength, it was not as effective in terms of the toughness. It was reported that additional Mo improves the toughness of SA508 Gr.3 Mn–Mo–Ni low alloy steel due to the enhancement of the fine M_2C precipitation as opposed to coarse cementite, which precipitates between the bainitic ferrite laths and reduces the toughness of the steel significantly [1,17]. However, effective carbide size refinement with an addition of Mo was not observed in the case of the SA508 Gr.4N Ni–Mo–Cr low alloy steel due to its completely different carbide phase and morphology.

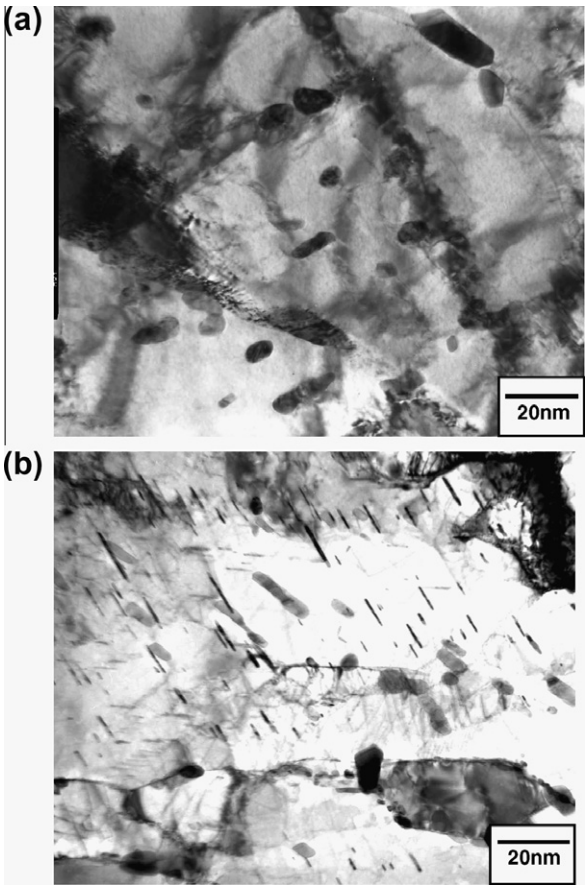

Fig. 7. Carbide distribution observed by TEM: (a) K4-Mo1 and (b) K4-Mo2.

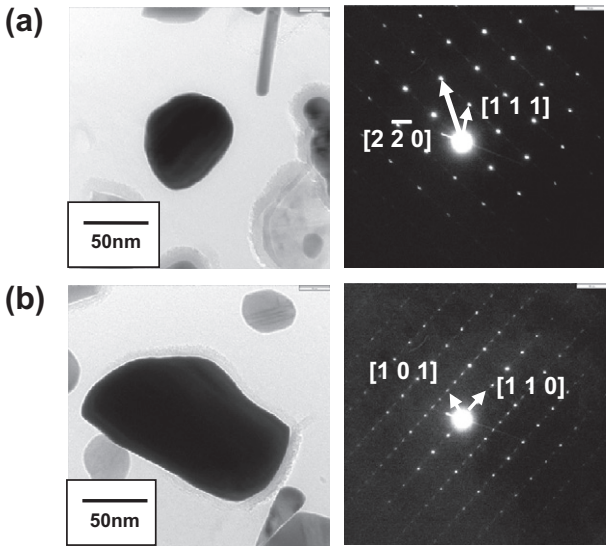

Fig. 8. Diffraction patterns of the precipitates: (a) $M_{23}C_6$, (b) M_7C_3.

3.5. Correlation between the thermodynamic calculation and experimental results

In the previous section, it was concluded that the change of the stable phase is closely associated with the change of microstructure, which is especially true for the change in the precipitation behavior. In addition, these properties were found to be related

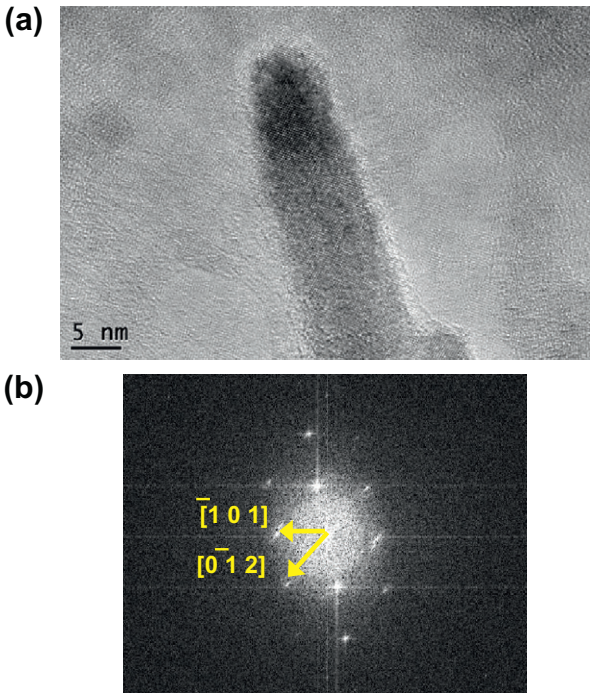

Fig. 9. HREM images of M_2C carbide and its converted diffraction pattern by Fourier transformation: (a) HR image of M_2C, (b) converted diffraction pattern.

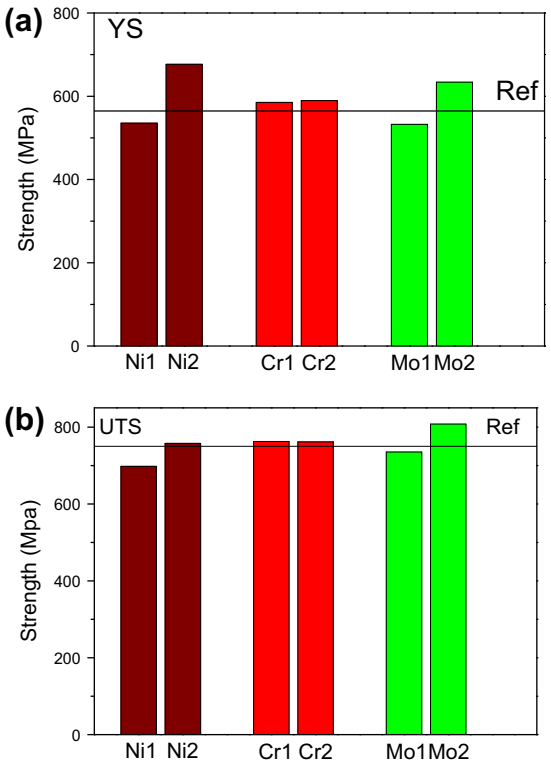

Fig. 10. Tensile properties of the model alloys: (a) Yield strength, (b) Tensile strength.

to the mechanical properties. For this reason, the change in the microstructure (especially the change of the precipitation behavior) and the mechanical properties of Ni–Mo–Cr low alloy steel with different Cr and Mo contents may be deduced from the thermodynamic calculation results. The calculation results with variation of Cr and Mo contents are shown in Fig. 12 [28].

Table 3
Mechanical properties of model alloys.

	YS (MPa)	UTS (MPa)	EL (%)	T_{41J} (°C)	T_{68J} (°C)	USE (J)
K4-Ref	580	750	18	−127	−111	224
K4-Ni1	530	700	17	−88	−78	263
K4-Ni2	680	760	17	−160	−138	207
K4-Cr1	585	760	17	−65	−49	189
K4-Cr2	590	760	16	−139	−123	216
K4-Mo1	530	735	17	−138	−121	243
K4-Mo2	650	805	15	−122	−101	184

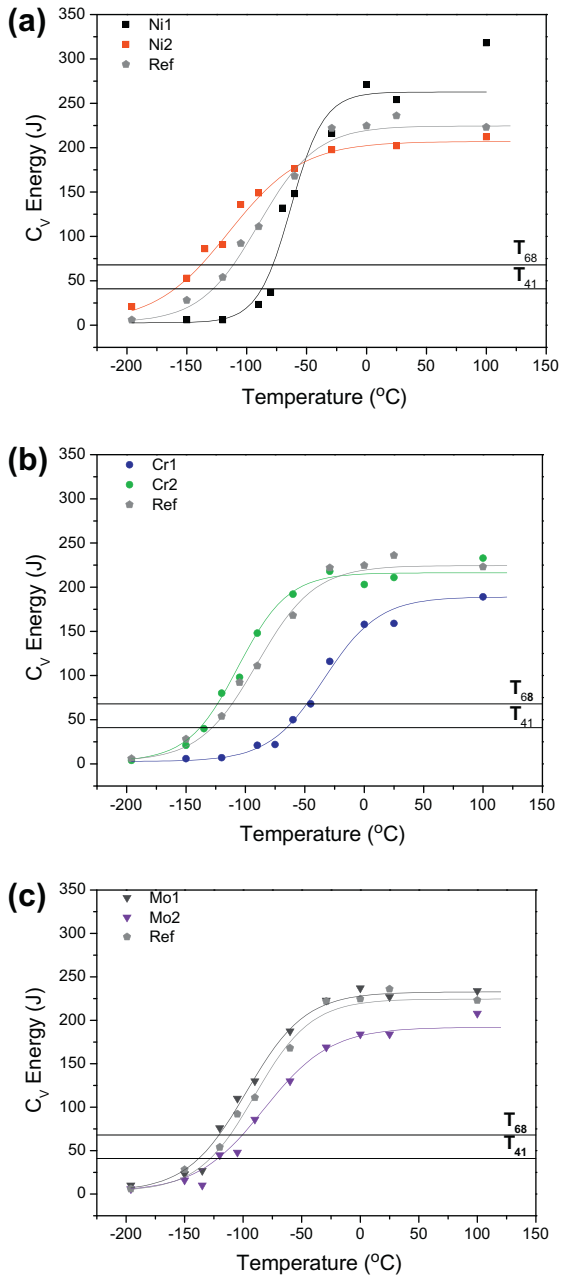

Fig. 11. Charpy impact energy transition curves of the model alloys: (a) Ni effects, (b) Cr effects and (c) Mo effects.

In the region of 1.0 wt% of Cr, M_7C_3 represents the only stable carbide phase in 0.1 wt% Mo. Its fraction decreases as well and shows a sigmoidal shape at approximately 500 °C. When the Mo content is increased to 0.5 wt%, the $M_{23}C_6$ phase appears with the M_7C_3 phase, and both fractions of the phases are also decreased, showing a sigmoidal shape in the temperature range close to 500 °C. These types of reductions of the carbide fraction result in carbide coarsening, as observed in the microstructure of K4-Cr1. This will lower the transition behavior of the model alloys.

When the Mo content exceeds 1.0 wt%, the M_2C carbide phase appears with $M_{23}C_6$ in the range of 1.0–1.8 wt% Cr, and M_2C precipitates in the low alloy steel. This will increase the strength of the model alloy while it lowers the toughness due to the hardening of the precipitation. However, the M_2C phase disappears as the Cr content increases to 2.5 wt%, and the $M_{23}C_6$ carbide becomes the only stable phase in this system. As we observed before, the mean size of the $M_{23}C_6$ and M_7C_3 carbides in K4-Ref are about 250–350 nm, and they distributed homogeneously in both boundaries and inside the grains. In addition, there are no big differences in morphology between $M_{23}C_6$ and M_7C_3 carbides. Hence, though the 1.0 wt% Mo and 2.5 wt% Cr does not have M_7C_3, overall precipitation behavior (size and distribution) will be similar to that of K4-Ref. In the region of 2.5 wt% of Cr, the behaviors of carbide phases varied depending on the Mo content. The M_7C_3 phase is the only stable phase in the case of 0.1 wt% Mo initially. However, the M_7C_3 phase grows gradually unstable and its fraction is reduced with an increase of the Mo content, as shown with 0.5 wt% Mo. In contrast, the stability of the $M_{23}C_6$ phase is enhanced and the $M_{23}C_6$ phase appears with the M_7C_3 phase with 0.5 wt% Mo. Finally, with 1.0 wt% Mo, the M_7C_3 phase disappears and the $M_{23}C_6$ carbide is the only stable phase. Though the types of stable carbide phases change depending on the Mo content, the model alloys with 0.1–1.0 wt% Mo will show precipitation behavior that is similar to that of K4-Ref due to the similar size and distribution of M_7C_3 and $M_{23}C_6$. Moreover, it is expected that these model alloys also show transition characteristics that are similar to those of K4-Ref due to the similarity of precipitation behavior. The changes in the precipitation behavior and mechanical properties with changes of the Cr and Mo contents are summarized in Fig. 13.

4. Conclusions

The microstructure and mechanical properties in SA508 Gr.4N low alloy steel with different Ni, Cr contents were evaluated.

(1) From the results of the thermodynamic calculations and microstructure observations, the addition of Ni mainly affects the matrix, whereas it has little effect on the precipitation behavior. The strength of the alloys was increased with an increase of the Ni content as a result of both solid solution strengthening and a reduction of the subgrain size. The addition of Ni is the most effective method for improving both the strength and toughness of low alloy steel. Ni creates a solid solution with the ferrite matrix and improves the intrinsic toughness of the ferrite.
(2) Cr additions mostly affect the precipitation behavior. An addition of Cr suppresses the precipitation of cementite, reduces the carbide size, and distributes the carbides homogeneously. However, additional Cr causes a slight difference in the strength of the alloy. The variation of the Cr content affects the Charpy impact property by changing the precipitation behavior. Carbide coarsening occurred in low-Cr model alloy, which lowered the transition property.
(3) An addition of Mo decreases the stability of M_7C_3 and enhances the precipitation of the fine needle-type M_2C carbide. The strength of the alloys was increased with an increase of the Mo content. An addition of Mo strengthens low alloy steel due to a combination of a solid solution hardening effect and a precipitation hardening effect. Mo also

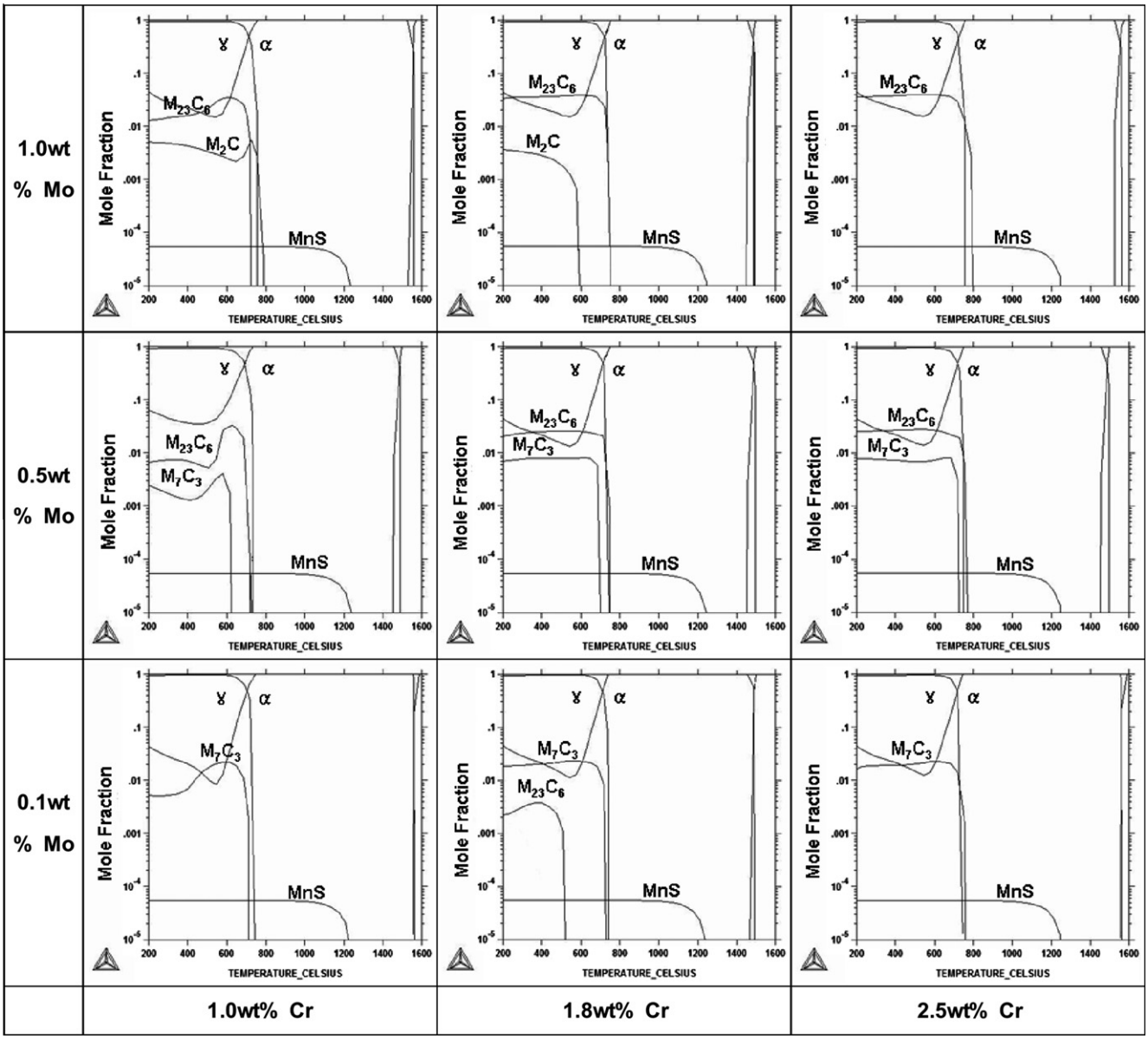

Fig. 12. Thermodynamic calculation results with various Cr and Mo contents [28].

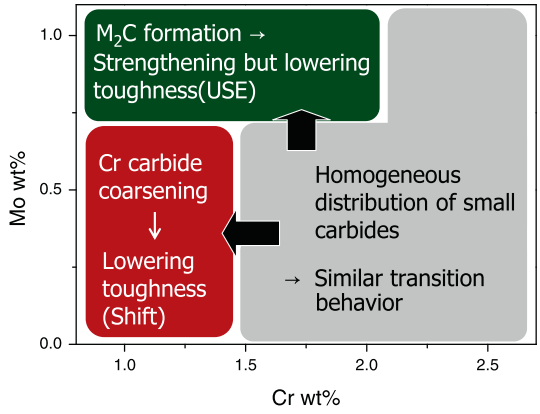

Fig. 13. Change of microstructure and mechanical properties of SA508 Gr.4N low alloy steel change with Cr and Mo contents.

affects the Charpy impact property by changing the precipitation behavior, though it is less effective than Ni and Cr.

(4) The changes in the microstructure and mechanical properties were correlated with the thermodynamic calculations. The change in both the precipitation behavior and the mechanical properties caused by variation of the Cr and Mo contents could be estimated by the thermodynamic calculation results.

Acknowledgement

This study was carried out under the Nuclear R&D program of the Ministry of Knowledge Economy of Korea.

References

[1] P. Bowen, S.G. Druce, J.F. Knott, Acta Metall. 34 (1986) 1121.
[2] M.C. Kim, Y.J. Oh, J.H. Hong, Scripta Mater. 43 (2000) 205.
[3] K. Suzuki, I. Sato, H. Tsukada, Nucl. Eng. Des. 151 (1994) 513.
[4] N. Ohashi, T. Enami, H. Wanaka, K. Aso, Nucl. Eng. Des. 81 (1984) 193.
[5] S.G. Druce, B.C. Edwards, Nucl. Energy 19 (1980) 347.
[6] Y.R. Im, Y.J. Oh, B.J. Lee, J.H. Hong, H.C. Lee, J. Nucl. Mater. 297 (2001) 138.

[7] A.V. Nikolaeva, Y. Nikolaaeva, J. Nucl. Mater. 218 (1994) 85.
[8] A.M. Kryukov, Y.A. Nikolaev, Nucl. Eng. Des. 186 (1998) 353.
[9] L. Kaufman, H. Bernstein, Computer Calculation of Phase Diagrams, Academic Press, New York, 1970.
[10] W.F. Smith, Metals and Materials, Interversion Inc., 2003.
[11] S.H. Kim, Y.R. Im, S.H. Lee, H.C. Lee, Y.J. Oh, J.H. Hong, J. Kor. Inst. Metall. Mater. 38 (2000) 771.
[12] M. Tu, C. Hsu, W. Wang, Y. Hsu, Mater. Chem. Phys. 107 (2008) 418.
[13] B.Y. Kang, H.J. Kim, S.K. Hwang, ISIJ Int. 12 (2000) 1237.
[14] W. Jolley, J. Iron Steel Inst. 206 (1968) 170.
[15] B.V. Narasimha Rao, G. Thomas, Metall. Trans. A 11A (1980) 441.
[16] G. Thomas, Transmission Electron Microscopy of Materials, Techbooks, Inc., 1990.
[17] Research Report, KAERI/CM-785/2004.
[18] S. Takeuchi, J. Phys. Soc. Jpn. 27 (1969) 929.
[19] W.C. Leslie, Metall. Trans. 3 (1972) 5.
[20] S.G. Song, H. Du, E.Y. Sun, Metall. Mater. Trans. A 33A (2002) 1963.
[21] J.W. Martin, Precipitation Hardening, Butterworth-Heinemann, 1998.
[22] W. Jolley, Trans. TMS-AIME 242 (1968) 306.
[23] J. Naylor, R. Blondeau, Metall. Trans. A. 7A (1976) 891.
[24] M.K. Shin, J.H. Cho, J. Kor. Inst. Metall. Mater. 16 (1978) 477.
[25] H. Kwon, C.H. Kim, Metall. Trans. A 17A (1986) 1173.
[26] C.H. Yoo, H.M. Lee, C.G. Kim, J. Kor. Inst. Metall. Mater. 33 (1995) 10.
[27] G.P. Gibson, M. Caple, S.G. Druce, Defect Assessment in Components, Mechanical Engineering Publications, Inc., 1991.
[28] S.G. Park, M.C. Kim, B.S. Lee, D.M. Wee, J. Kor. Inst. Metall. Mater. 46 (2008) 771.